Biosensors and Bioelectronics 53 (2014) 399–405

Contents lists available at ScienceDirect

Biosensors and Bioelectronics

journal homepage: www.elsevier.com/locate/bios

Highly sensitive and label-free electrochemical detection of microRNAs based on triple signal amplification of multifunctional gold nanoparticles, enzymes and redox-cycling reaction

Lin Liu [a,*], Ning Xia [a,b], Huiping Liu [a], Xiaojing Kang [a], Xiaoshuan Liu [a], Chan Xue [a], Xiaoling He [a]

[a] College of Chemistry and Chemical Engineering, Anyang Normal University, Anyang, Henan 455000, People's Republic of China
[b] College of Chemistry and Chemical Engineering, Central South University, Changsha, Hunan 410083, People's Republic of China

ARTICLE INFO

Article history:
Received 31 July 2013
Received in revised form
2 October 2013
Accepted 11 October 2013
Available online 23 October 2013

Keywords:
MicroRNAs
Triple signal amplification
Redox cycling
Gold nanoparticles
Alkaline phosphatase
Electrochemical genosensors

ABSTRACT

MicroRNAs (miRNAs) are believed to be important for cancer diagnosis and prognosis, serving as reliable molecular biomarkers. In this work, we presented a label-free and highly sensitive electrochemical genosensor for miRNAs detection with the triple signal amplification of gold nanoparticles (AuNPs), alkaline phosphatase (ALP) and p-aminophenol (p-AP) redox cycling. The label-free strategy is based on the difference in the structures of RNA and DNA. Specifically, miRNAs were first captured by the pre-immobilized DNA probes on a gold electrode. Next, the cis-diol group of ribose sugar at the end of the miRNAs chain allowed 3-aminophenylboronic acid (APBA)/biotin-modified multifunctional AuNPs (denoted as APBA–biotin–AuNPs) to be attached through the formation of a boronate ester covalent bond, which facilitated the capture of streptavidin-conjugated alkaline phosphatase (SA–ALP) via the biotin–streptavidin interaction. After the addition of the 4-aminophenylphosphate (p-APP) substrate, the enzymatic conversion from p-APP to p-AP occurred. The resulting p-AP could be cycled by a chemical reducing reagent after its electro-oxidization on the electrode (known as p-AP redox cycling), thus enabling an increase in the anodic current. As a result, the current increased linearly with the miRNAs concentration over a range of 10 fM–5 pM, and a detection limit of 3 fM was achieved. We believe that this work will be valuable for the design of new types of label-free and sensitive electrochemical biosensors.

© 2013 Elsevier B.V. All rights reserved.

1. Introduction

MicroRNAs (miRNAs) are 18- to 25-nucleotide-long non-coding RNA molecules that play roles in developmental and cell biology, including developmental regulation, stress responses, cell differentiation, cardiogenesis and epigenetic inheritance. Recently, the aberrant expression of miRNAs has been correlated with cancer (prostate, breast, colon, lung, etc.) and other diseases (diabetes, heart diseases, etc.), making miRNAs clinically important biomarkers and drug discovery targets (Dong et al., 2013; Tran et al., 2013). The methods currently used for miRNAs detection, such as Northern blotting, microarrays and polymerase chain reaction (PCR), are usually time-consuming, less sensitivity and/or require fluorescent- or radio-labeling and complicated instrumentation (Nelson et al., 2004; Schmittgen et al., 2004; Streit et al., 2009). Therefore, it is critical to develop robust detection methods for miRNAs with high sensitivity, selectivity and simplicity (Cissell et al., 2007; Zhang et al., 2009).

In recent years, electrochemical genosensors have held great promise as devices suitable for point-of-care diagnostics and multiplexed platforms for fast, simple and inexpensive nucleic acid analysis (Paleček and Bartošík, 2012). A typical electrochemical genosensor is made of a solid electrode with an immobilized short single-stranded nucleotide probe for hybridization with the complementary sequence (Lu et al., 2008a; Tosar et al., 2010; Xie et al., 2004). Once hybridization occurs, there must be a way to translate the hybridization event into a measurable signal. One of the limiting factors for the development of electrochemical miRNAs sensors is sensitivity, as the miRNAs content is at the attomolar to femtomolar level in biological samples (Cissell et al., 2007). Recently, great efforts have been made to develop sensitive electrochemical genosensors for the detection of low-abundance miRNAs (Dong et al., 2012; Gao et al., 2013; Gao and Yu, 2007; Gao and Yang, 2006; Hong et al., 2013; Kilic et al., 2012, 2013; Lusi et al., 2009; Pöhlmann and Sprinzl, 2010; Peng and Gao, 2011; Ren et al., 2013; Shen et al., 2013; Wang et al., 2013; Yin et al., 2012b). Signal amplification is the most popular strategy for the development of ultrasensitive assay methods (Duan et al., 2013). Normally, signal amplification can be achieved using a nanoparticle or enzyme catalytic reaction (single amplification)

* Corresponding author. Tel.: +86 732 2900040.
E-mail address: liulin@aynu.edu.cn (L. Liu).

0956-5663/$ - see front matter © 2013 Elsevier B.V. All rights reserved.
http://dx.doi.org/10.1016/j.bios.2013.10.026

or a nanoparticle/enzyme conjugate catalytic reaction (double amplification). These methods often require the labeling of nanoparticles with complementary probes for the recognition of miRNAs or the use of labeled DNA/RNA for a competitive binding assay. The practical applications of these methods are therefore limited due to their time-consuming and costly preparation, the instability of the modified nanoparticle, and their low sensitivity for real sample assays.

A more recent approach for signal amplification is to employ multiple signal amplification, such as a catalytic reaction plus a redox-cycling reaction (Yang, 2012). In redox cycling, electrochemically oxidized (or reduced) species are reduced (or oxidized) electrochemically, enzymatically, or chemically. The regenerated electroactive species are electrochemically re-oxidized (or re-reduced), resulting in high electrochemical signals. For example, Das et al. (2006) and Tang et al. (2011) suggested that antibody-coated gold nanoparticles (AuNPs) can improve the sensitivity of electrochemical immunoassays using p-aminophenol (p-AP) redox cycling. Yang's group reported a series of chemical amplification approaches using an enzymatic reaction and electrochemical–chemical redox cycling by different reducing reagents on indium-tin oxide (ITO) electrodes (Akanda et al., 2011, 2012, 2013; Das et al., 2007). These electrochemical immunoassays allow low-concentration proteins (femtomolar or below) to be detected readily.

The hydroxyl group at the 2′ position of the ribose sugar provides the RNA molecule with a cis-diol group at the 3′-terminal. This property enables miRNAs to be distinguished from DNA. For example, based on the difference in the structures of RNA and DNA, Gao's group developed an electrochemical biosensor for miRNAs detection using OsO_2 nanoparticles as tags for miRNAs labeling (Gao and Yang, 2006). Paleček's group demonstrated that the 3′-end of miRNAs can be selectively modified with Os(VI)2,2′-bipyridine (Trefulka et al., 2010). Phenylboronic acids can form boronate ester covalent bonds with diol-containing biomolecules (e.g., dopamine, sugars, nucleosides, antibodies and glycoproteins) (Abad et al., 2002; Frasconi et al., 2010; Ho et al., 2010; Lin et al., 2009, 2011; Liu et al., 2013b; Song et al., 2012; Xia et al., 2013a). The capture, separation and immobilization of nucleotides and RNA with boronic-acid-functionalized materials have also been achieved by several groups (Deore and Freund, 2005; Li et al., 2011; Pham et al., 2010; Potter et al., 2006; Rahman and Elaissari, 2012; Zayats et al., 2002). Recently, our group reported a label-free strategy for miRNAs detection based on the dual amplification of 4-mercaptophenylboronic acid (MBA)-capped and dopamine (DA)-modified AuNPs (Xia et al., 2013b). As a result, a detection limit of 50 fM was achieved. In the present work, we developed a highly sensitive and label-free electrochemical method for miRNAs detection based on the triple signal amplification of multifunctional AuNPs, alkaline phosphatase (ALP) and p-AP redox-cycling reaction. Specifically, miRNAs captured by the DNA probes on a gold electrode were derivatized with 3-aminophenylboronic acid/biotin-modified multifunctional AuNPs through the formation of boronate ester covalent bonds. The derivation allowed streptavidin-conjugated alkaline phosphatase (SA–ALP) to be attached for the production of electrochemically active p-AP. The produced p-AP could be cycled by a chemical reducing reagent after its electrooxidization on the electrode, increasing the anodic current.

2. Experimental

2.1. Chemicals and reagents

Tris(carboxyethyl)phosphine (TCEP), 6-mercapto-1-hexanol (MCH), 3-aminophenylboronic acid (APBA) hydrochloride, streptavidin-conjugated alkaline phosphatase (SA–ALP), bovine serum albumin (BSA), 1-ethyl-3-[3-dimethylaminopropyl]carbodiimide hydrochloride (EDC), KH_2PO_4, K_2HPO_4, trisodium citrate and tris-(hydroxymethyl)aminomethane hydrochloride (Tris–HCl) were purchased from Sigma-Aldrich. 4-Aminophenylphosphate (p-APP) was obtained from Enzo Life Sciences, Inc. (Farmingdale, NY, USA). Diethylpyrocarbonate, adenosine-5′-monophosphate (AMP), cytosine-5′-monophosphate (CMP) and a thiolated single-stranded DNA (ss-DNA) probe (5′-TCAACATCAGTCTGATAAGCTA-$(CH_2)_6$-SH-3′) were purchased from Sangon Biotech. Co., Ltd. (Shanghai, China). The target miRNA-21 and the mismatch sequences were obtained from GenePharma Co., Ltd. (Shanghai, China) with the following sequences: 5′-UAGCUUAUCAGACUGAUGUUGA-3′ (miRNA-21), 5′-UAGCUUAUCGGACUGAUGUUGA-3′ (single-based mismatch), 5′-UUGCUUAUCGGACUGAUCUUGA-3′ (three-based mismatch) and 5′-GUAAGGCAUCUGACCGAAGGCA-3′ (non-complementary). The peptides (CALNN and CALNNGK(biotin)G) were synthesized and purified by ChinaPeptides Co., Ltd. (Shanghai, China). All other reagents were purchased from Beijing Chemicals, Ltd. (Beijing, China). The DNA solutions were prepared using TE buffer solution (10 mM Tris–HCl, 1 mM EDTA, pH 7.4), and kept at −18 °C. The miRNAs stock solutions were prepared daily with diethylpyrocarbonate-treated water in an RNase-free environment. The hybridization solution was prepared with TNE buffer (TE+0.1 M NaCl). The buffer (EB) for the electrochemical experiment was 10 mM Tris, 1 mM $MgCl_2$ and 50 mM Na_2SO_4 (pH 7.4).

2.2. Formation of boronate esters between the nucleotide and APBA

The formation of boronate esters between nucleotide and APBA was confirmed by mass spectroscopy (LCT Premier XE). APBA and the nucleotide (AMP or CMP) were dissolved in deionized water at 100 and 20 μM, respectively. The pH of the APBA/nucleotide mixed solution was then adjusted to 8.0 with 1 M NaOH and the mass spectra were collected in negative ion mode.

2.3. Synthesis and characterization of multifunctional AuNPs

All glassware used in the following procedure was cleaned in a bath of freshly prepared 1:3 HNO_3–HCl, rinsed thoroughly with water and dried in air prior to use. The peptide-functionalized AuNPs (denoted as biotin–AuNPs) were prepared by ligand-exchange reaction between CALNN and CALNNGK(biotin)G peptides and citrate-stabilized AuNPs, as in previous reports (Lévy et al., 2004; Wang et al., 2005). Briefly, trisodium citrate (5 mL, 38.8 mM) was rapidly added to a boiling solution of $HAuCl_4$ (50 mL, 1 mM), and the solution was boiled continually for an additional 30 min to yield a red-wine-colored solution. The particle concentration of the synthesized AuNPs suspension was determined to be 10.2 nM based on a molar absorptivity of $2.7 \times 10^8\ M^{-1}\ cm^{-1}$ at 520 nm. The ligand-exchange reaction was then performed at room temperature by mixing 5 mL of the as-prepared AuNPs suspension with CALNN and CALNNGK(biotin)G at room temperature for 2 h. The concentration ratio of CALNN to CALNNGK(biotin)G was 9:1, as in the previous study (Lévy et al., 2004). The immobilization ability of AuNPs for the peptides was studied by measuring the free peptides in solution with mass spectroscopy. The results indicated that CALNN and CALNNGK (biotin)G molecules at concentrations of 6.3 and 0.7 μM were almost completely absorbed by the 10.2 nM AuNPs suspension (see Fig. S1 in Supplementary material). Thus, the average number of CALNN and CALNNGK(biotin)G molecules per gold nanoparticle was estimated to be 618 and 69, respectively. The suspension was thoroughly rinsed with deionized water to remove the lower amounts of free peptides. The 3-aminophenylboronic acid (APBA)-modified biotin–AuNPs (denoted as APBA–biotin–AuNPs) were prepared by cross-linking APBA molecules onto the biotin–AuNPs surface via the EDC-mediated amine coupling reaction

(Kanayama and Kitano, 2000; Liu et al., 2013a; Moreno-Guzmán et al., 2012; Zayats et al., 2002). Biotin–AuNPs were mixed with a solution comprised of 50 μM EDC and 1 μM APBA at pH 7.4 for 6 h, which was followed by three repetitions of centrifugation and re-dispersion in 1 mM phosphate-buffered saline solution (PBS, pH 7.4). The number of APBA molecules capped on EDC-activated AuNPs was determined by measuring the remaining APBA in solution with mass spectroscopy. The results indicated that each gold nanoparticle was capped with 30 APBA molecules (Fig. S2). The synthesized AuNPs were characterized using a Cary 50 spectrophotometer and an FEI Tecnai G2 T20 transmission electron microscope (TEM).

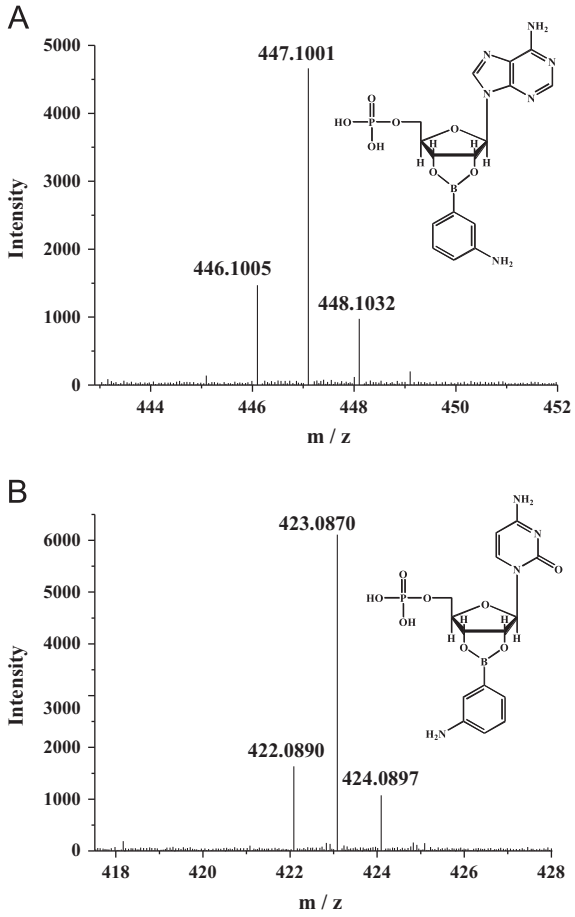

Fig. 1. Mass spectra of the APBA–AMP (A) and APBA–CMP (B) complexes.

2.4. Procedure for miRNAs detection

A 2-mm-diameter gold disk electrode was polished with 0.05-μm alumina, sonicated in ethanol and water and dried with nitrogen. Next, the cleaned gold electrode was immersed in a solution of 1.0 μM thiolated ssDNA containing 5 μM TCEP in the darkness for 12 h. This step was followed by washing the electrode thoroughly with water and soaking it in a 0.1 mM MCH solution for 5 min and a 1% BSA solution for 30 min to block the unreacted gold surface. The use of the mixed self-assembled monolayer (SAM) of thiolated DNA and MCH eliminates the nonspecific adsorption of DNA/RNA on the gold surface and orients the pre-immobilized DNA molecules for more efficient hybridization (Dong et al., 2012; Johnson and Mutharasan, 2012). Next, 10 μL of TNE containing a given concentration of miRNAs was cast onto the electrode surface for the hybridization between miRNAs and pre-immobilized DNA probe for 30 min, as in the previous reports (Dong et al., 2012; Xia et al., 2013b). Again, the electrode was rinsed with water to remove any non-specifically adsorbed substance. To attach SA–ALP, the electrode was first allowed to react with 10 μL of the APBA–biotin–AuNPs suspension for 30 min, and then exposed to 10 μL of the SA–ALP solution for 10 min. After the electrode was washed with water to remove the excess physiadsorbed SA–ALP, the electrode was immersed in the EB solution containing 0.5 mM p-APP and 2 mM TCEP for 30 min in a 30 μL homemade plastic electrochemical cell. Finally, voltammetric and amperometric detection of p-AP in the redox cycling was carried out on a DY2013 electrochemical workstation (Digi-Ivy, Inc., Austin, TX) with a platinum wire and a Ag/AgCl electrode as the auxiliary and the reference electrode, respectively.

3. Results and discussion

3.1. Principle of the method for miRNAs detection

The labeling of DNA or miRNAs with nanoparticles offers better selectivity and sensitivity, but there are some limitations to the extensive application of labeled DNA or miRNAs due to its high operational complexity and cost. Label-free biosensors are important due to their simplicity, convenience and low cost. The label-free strategy of our method is based on the difference in the structure of RNA versus DNA and the formation of boronate ester covalent bonds between boronate moieties and cis-diols in nucleosides. The specific binding of phenylboronic acid to ribose sugar in ribonucleotides has been demonstrated in previous reports (Deore and Freund, 2005; Kanekiyo et al., 2004; Shimomura et al., 2003). Herein, the complexes

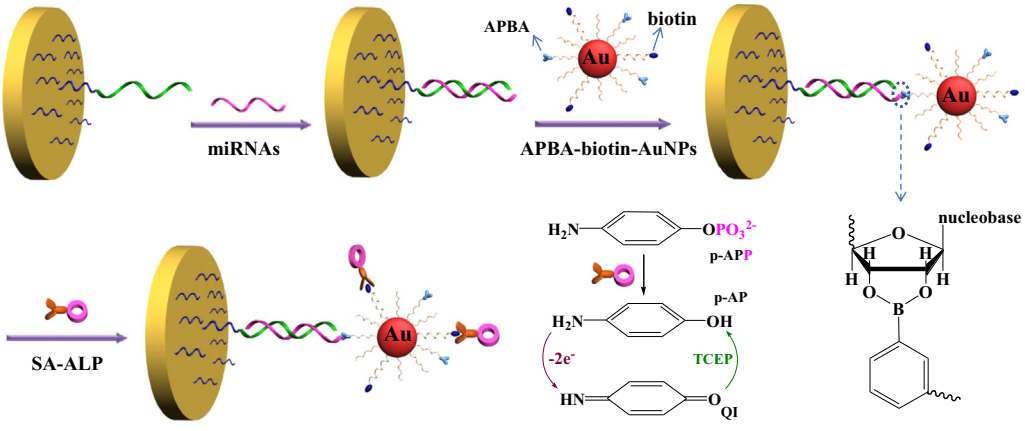

Fig. 2. Schematic representation of the label-free detection of miRNAs based on the triple signal amplification of APBA–biotin–AuNPs, SA–ALP and the p-AP redox-cycling reaction.

between nucleosides and APBA were first characterized using mass spectrometry. As shown in Fig. 1, the dominant mass peaks at 447.1001 Da (Fig. 1A) and 423.0870 Da (Fig. 1B) correspond to the complexes of APBA–AMP and APBA–CMP, respectively.

The analytical principle behind the miRNAs detection method is shown in Fig. 2. Target miRNAs are captured by DNA probes immobilized on a gold electrode via the hybridization reaction. The cis-diol of ribose sugar in miRNAs allows APBA–biotin–AuNPs to be attached through the formation of boronate ester covalent bonds. Furthermore, the attachment of APBA–biotin–AuNPs facilitates the capture of SA–ALP conjugates via the biotin–streptavidin interaction. After the addition of the p-APP substrate, the enzymatic reaction from p-APP to p-AP proceeds. In this process, the auto-oxidization of enzymatically generated p-AP could be prevented by TCEP. This step is followed by the electrochemical detection of the generated p-AP in the presence of TCEP. This method will be highly sensitive because: (1) a biotin-modified gold nanoparticle can attach more than one SA–ALP molecule, (2) each SA–ALP molecule can catalyze the production of a large number of electrochemically active p-AP molecules due to its high turnover frequency and high reaction selectivity, and (3) the produced p-AP is cycled by TCEP after its electro-oxidization on the electrode, enabling the increase of the anodic current. Note that other strong reductants, such as hydrazine, sodium borohydride and nicotinamide adenine dinucleotide (NADH), have also been used in p-AP redox cycling and show good performance in immunosensor on ITO electrodes (Akanda et al., 2011, 2012, 2013; Das et al., 2007). Herein, we chose TCEP as the reducing reagent because TCEP is highly water soluble and stable in air, rapidly reduces the oxidized p-AP and has a low background current on SAM-covered gold electrodes (Akanda et al., 2011; Liu et al., 2014).

3.2. Characterization of APBA–biotin–AuNPs

In nanoparticle-based electrochemical biosensors, nanoparticles are usually used to enhance the biosensor sensitivity by increasing the loading of the enzymes or electrochemically detectable species or catalyzing the electrolysis of large concentrations of substrate. Recently, the modification of AuNPs with multiple functionalities has great value because it provides increased flexibility for multiplexing in bioanalytical applications and new tools for controlling the bottom-up assembly of nanostructures. In this work, AuNPs were capped with CALNN and CALNNGK(biotin)G peptides (denoted as biotin–AuNPs). These modified AuNPs are readily prepared, water-soluble and extremely stable over long storage periods and show no indication of nonspecific binding on DNA-covered surface (Wang et al., 2005). Moreover, the biotin groups on the AuNPs surface facilitate the conjugation of streptavidin through the biotin–streptavidin interaction. Previously, it was reported that each gold nanoparticle can attach 791∼919 peptide (CALNN) molecules (Lévy et al., 2004). In this work, the average numbers of CALNN and CALNNGK(biotin)G molecules per gold nanoparticle were determined to be approximately 618 and 69, respectively (Fig. S1). The APBA modification was performed by cross-linking APBA molecules onto the AuNPs via the EDC-mediated amine coupling reaction. We also found that the positively charged EDC could induce the aggregation of citrate-stabilized AuNPs, while the peptide-modified AuNPs were extremely stable in the presence of EDC. The modified AuNPs were characterized by UV–vis spectroscopy and TEM. As shown in Fig. 3, the modified and unmodified AuNPs display a characteristic UV–vis absorption spectrum with a plasmon band at 520 nm, which was ascribed to the surface plasmon resonance of the AuNPs. The formation of a peptide layer on the surface of the nanoparticles did not cause any apparent shift of the plasmon band absorbance, which is in agreement with previous findings (Lévy et al., 2004).

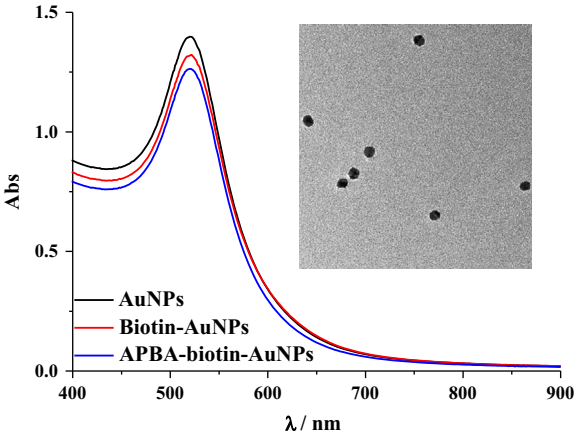

Fig. 3. UV/vis absorption spectra of the modified and unmodified AuNPs. The inset shows the TEM image of the synthesized APBA–biotin–AuNPs.

The slight decrease in the absorption of modified AuNPs is attributed to the loss of AuNPs during the repeated centrifugation and re-dispersion. Furthermore, the monodispersion of synthesized APBA–biotin–AuNPs was characterized by TEM. The average size of APBA–biotin–AuNPs (∼13 nm) was close to that of biotin-AuNPs (13 nm) and AuNPs (12.4 nm).

3.3. Feasibility for miRNAs detection

MicroRNA-21 (miRNA-21) has been found to be upregulated under many pathological conditions, including cancer and cardiovascular diseases (Lu et al., 2008b). Interest in miRNA-21 detection has dramatically increased during recent years (Dong et al., 2012; Kilic et al., 2012; Lee and Jung, 2011; Yin et al., 2012b). As proof of our method, miRNA-21 was tested. The red and blue curves in Fig. 4A are the representative CVs collected at DNA/MCH-covered electrode with the capture of miRNA-21, the subsequent attachment of APBA–biotin–AuNPs and SA–ALP and then the incubation with p-APP. Without TCEP, the response is only produced by the electro-oxidization of enzymatically generated p-AP (blue curve), as no redox peak was observed in the absence of SA–ALP. Upon the addition of TCEP, the anodic current was greatly enhanced (red curve), showing signal amplification by the redox cycling. For the experiment in which miRNA-21 was not introduced to the electrode, no peak was observed (black curve). The results demonstrated that the attachment of APBA–biotin–AuNPs is dependent upon miRNA-21 and that the immobilization of SA–ALP is dependent on the anchored APBA–biotin–AuNPs. We also investigated the effect of the SA–ALP and p-APP concentrations on the oxidation current, and found that the current increased with increasing SA–ALP and p-APP concentration and then began to plateau beyond 0.56 U mL^{-1} and 0.2 mM, respectively (Fig. S3). The control experiment was implemented with biotin–AuNPs instead of APBA–biotin–AuNPs. The absence of any discernible peak in the green curve indicates that the recognition of miRNA-21 is strongly dependent upon the interaction between cis-diols in the ribose sugars and boronic acid moieties on AuNPs. The results also demonstrated that boronic acid groups were successfully introduced onto the surface of AuNPs through the EDC-mediated amine coupling reaction. The performance of the sensor was further evaluated by chronoamperometry, a sensitive and well-established electrochemical technique widely used in electrochemical enzyme immunoassays and DNA hybridizations (Walter et al., 2011; Wang et al., 2013; Zhou et al., 2012a; Zhou et al., 2012b). As shown in Fig. 4B, the current in the absence of TCEP (blue curve) is lower than that in the presence of TCEP (red curve), demonstrating that the signal was indeed amplified by the

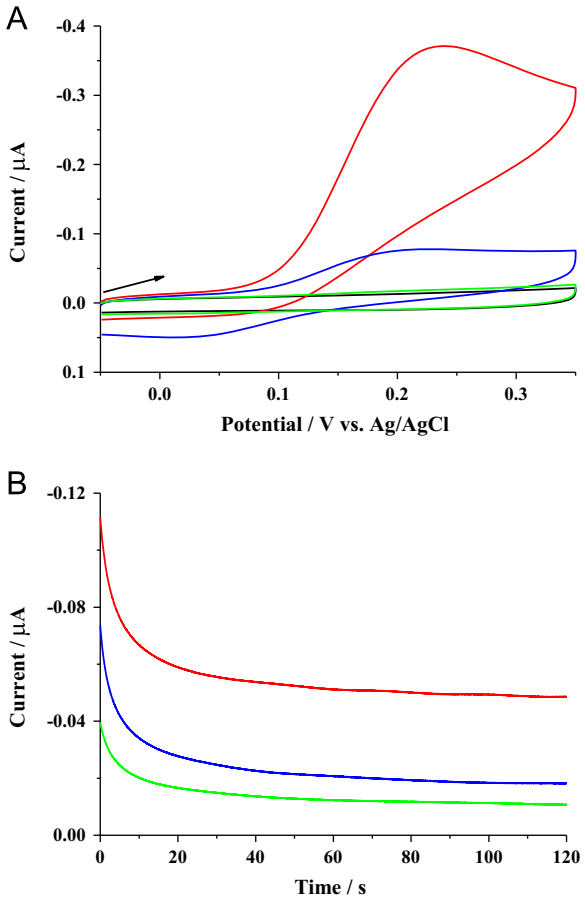

Fig. 4. Representative cyclic voltammograms (CVs) (A) and amperometric responses (B) acquired at DNA/MCH-covered electrodes after treatment with different procedures: red curve, miRNA-21 + APBA–biotin–AuNPs + SA–ALP + p-APP/TCEP; blue curve, miRNA-21 + APBA–biotin–AuNPs + SA–ALP + p-APP; green curve, miRNA-21 + biotin–AuNPs + SA–ALP + p-APP/TCEP; black curve, APBA–biotin–AuNPs + SA–ALP + p-APP/TCEP. The concentrations of miRNA-21, SA–ALP and p-APP were 10 pM, 2.33 U mL^{-1} and 0.5 mM, respectively. The scan rate in panel A was 20 mV/s and the current–time curves in panel B were obtained at a potential of 0.25 V. (For interpretation of the references to color in this figure legend, the reader is referred to the web version of this article.)

redox cycling. Moreover, the use of TCEP in this work could also prevent the atmospheric oxidation of p-AP and enable a longer incubation time.

A single gene can be simultaneously regulated by multiple miRNAs; thus, methods to detect multiple miRNAs are needed to fully understand the important and complex function of these tiny regulators. Considerable effort is being devoted to developing high-throughput analytical strategies for multiplexed miRNAs gene expression. For example, Northern blotting has been used as an efficient approach for multiplexed sample analysis, and oligonucleotide microarray-based detection platforms have been developed for high-throughput profiling. It is well known that double-stranded polynucleotides are susceptible to denaturation and that the boronate ester is unstable at low pH. We found that the electrode can be conveniently regenerated by rinsing the surface with a 10 mM HCl solution to desorb the target miRNAs and APBA–biotin–AuNPs. No obvious change in the current was observed after eight regeneration/assay cycles (Fig. S4). Thus, multiple samples can be determined using one electrode. We also found that the relative standard deviations (RSDs) are below 13% for three different electrodes in parallel, indicating that multiple electrodes can be prepared concurrently for the assay of many different samples. In addition, we studied the stability of the DNA/MCH-covered electrode. When stored in PBS at room temperature for one week, the sensor loses only 18% of its original signaling peak current (Fig. S5).

3.4. Sensitivity and selectivity to miRNA-21

miRNAs represent only a small fraction of the mass in total RNA sample; the miRNAs concentration in cells can be as low as a few molecules per cell. This low abundance requires a highly sensitive assay. Moreover, the expression level of miRNAs varies by as much as four orders of magnitude from a few copies to over 50,000 copies per cell; thus, a wide dynamic range of detection is also necessary (Dong et al., 2013). Having established the regeneration capability of the method, we assessed its other analytical merits, such as reproducibility, sensitivity and detection limit. The dependence of the amperometric currents on the miRNA-21 concentration is presented in Fig. 5A. The aforementioned regeneration of the sensor surface contributes to the good reproducibility of the method, as the RSDs are all less than 9.5% (Fig. 5B). The current increases linearly with the miRNA-21 concentration ranging from 10 fM to 5 pM and begins to level off beyond 10 pM. The linear regression equation is current (μA) = −0.007 [miRNA-21] (pM) − 0.012 (R^2 = 0.99). The detection limit of the method was estimated to be 3 fM (n = 11), which is lower than that achieved by AuNPs- and/or enzyme-based single or double signal amplification (Table 1) (Gao, 2012; Kilic et al., 2012; Wang et al., 2012; Xia et al., 2013b; Yin et al., 2012a, 2012b; Zhou et al., 2012a, 2012b). The lower detection limit is attributed to the electrocatalytic property of AuNPs, the high turnover frequency of alkaline phosphatase and the signal amplification of the p-AP redox-cycling reaction by TCEP. In addition, the multifunctional AuNPs are extremely stable and can react with miRNAs through the formation of boronate ester covalent bonds, facilitating the label-free detection of other miRNAs.

The small size and the sequence similarity of miRNAs in the RNA family greatly complicate miRNAs detection in situ based on hybridization reactions (Yang et al., 2009). When a sample is a mixture of pre- and mature miRNAs, the oligonucleotide probe can hybridize nonspecifically to pre-miRNAs. That is, a sequence mismatch can easily produce a false positive signal. Thus, strategies for improving the specificity of miRNAs profiling measurements are important and urgent. Herein, we also investigated the selectivity of the method to miRNA-21. As shown in Fig. 5C, the current in the case of non-complementary was close to the background level, but single- and three-base-mismatch miRNAs produced a positive signal at physiological temperature. Because of the difference of melting temperature (T_m), the discrimination of base mismatches depends on the hybridization temperature. For this reason, the interference of base-mismatch miRNAs could be eliminated by elevating the hybridization temperature (Lee and Jung, 2011; Wang et al., 2012). Recently, we found that no obvious difference was observed for miRNA-21 detection at 37 and 65 °C, while the current in the case of single- or three-base-mismatch miRNAs was near as low as the background level at 65 °C (Xia et al., 2013b). Thus, the selectivity of the method was evaluated at 65 °C. At this temperature, the currents generated by the single- and three-base-mismatch miRNAs were almost as low as the background level (Fig. 5C), implying that mismatch miRNAs were not captured by the probes at high temperature. Therefore, the interference of base-mismatch miRNAs can be eliminated by elevating the hybridization temperature.

4. Conclusion

In conclusion, we reported a highly sensitive and label-free electrochemical genosensor for miRNAs detection. Compared with

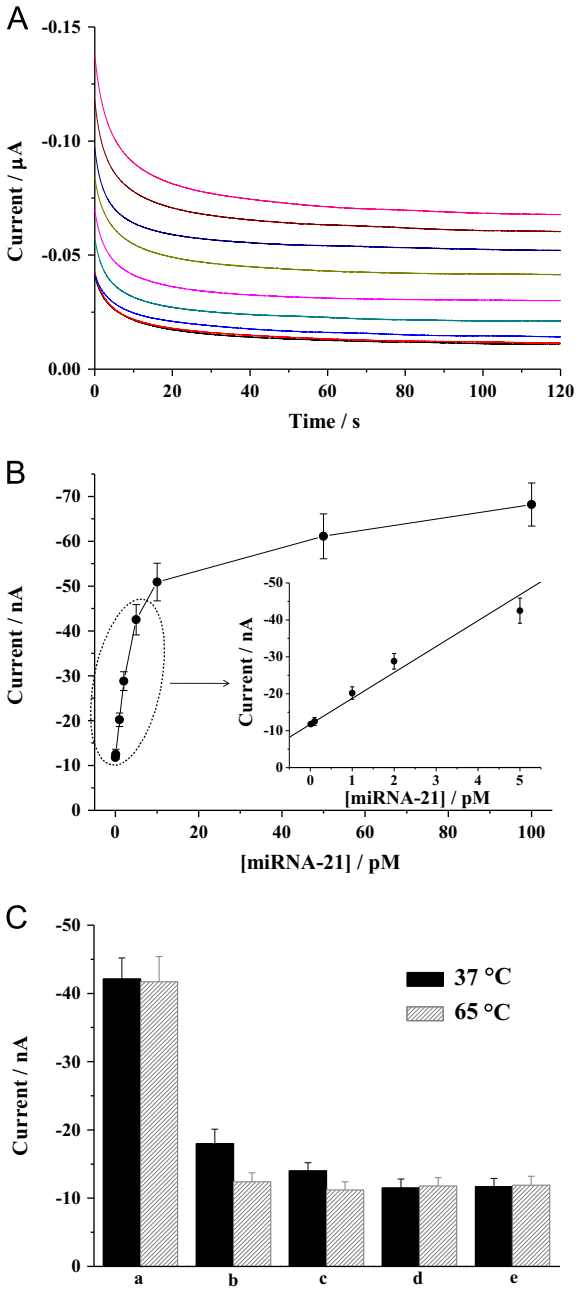

Fig. 5. (A) Amperometric responses at the sensing electrode with increasing miRNA-21 concentrations (from bottom to top: 0, 0.01, 0.1, 1, 2, 5, 10, 50 and 100 pM). (B) Dependence of the amperometric current collected at 100 s on the concentration of miRNA-21. Each point was averaged from three replicates, and the error bars show the absolute standard. (C) Sensor selectivity at different temperatures (a: miRNA-21; b: single-base mismatch; c: three-base mismatch; d: non-complementary; and e: the background). The concentrations of miRNAs used are 5 pM. The other experimental conditions are the same as those in Fig. 4.

other AuNPs- and enzyme-based electrochemical methods, our method has following advantages. First, the cis-diol at the 3′-terminal allows miRNAs molecules to be recognized by phenylboronic acid under mild conditions, facilitating label-free detection. Second, the multifunctional AuNPs are extremely stable and can be used to recognize all miRNAs sequences through the formation of boronate ester covalent bonds, allowing the obviation of the use of specific DNA/RNA modification for molecular recognition and signal amplification and reducing the operation complexity and the assay cost. Third, a relatively low detection limit (3 fM) was obtained because of the triple signal amplification of AuNPs, alkaline phosphatase and p-AP redox-cycling. We believe that our work will be valuable for the determination of miRNAs in a biological matrix and the design of new types of electrochemical biosensors for the sensitive detection of cis-diol-containing biomolecules.

Table 1
Comparison of the performance of electrochemical miRNAs sensors based on the signal amplification of AuNPs and/or enzymes.

Method of signal amplification	Detection limit	Linear range	References
SA–ALP	0.15 μM	Not reported	Kilic et al. (2012)
Glucose oxidase	4 fM	0.008–10 pM	Gao (2012)
Fc/SA–capped AuNPs	10 fM	0.01–2 pM	Wang et al. (2012)
Hemin-modified AuNPs	6 fM	5–5000 pM	Yin et al. (2012a)
MBA–AuNPs and DA–AuNPs	45 fM	0.1–10 pM	Xia et al. (2013b)
AuNPs/SA–HRP	0.4 pM	1–5000 pM	Zhou et al. (2012b)
AuNPs/SA–HRP	6 fM	0.01–700 pM	Zhou et al. (2012a)
Graphene/AuNPs/SA–HRP	60 fM	0.1–70 pM	Yin et al. (2012b)
AuNPs/SA–ALP/redox cycling	3 fM	0.01–5 pM	This work

Acknowledgments

Partial support of this work by the National Natural Science Foundation of China (Nos. 21205003, 21305004), the Joint Fund for Fostering Talents of National Natural Science Foundation of China and Henan Province (U1304205) and the Science & Technology Foundation of Henan Province (122102310517) is gratefully acknowledged.

Appendix A. Supplementary material

Supplementary data associated with this article can be found in the online version at http://dx.doi.org/10.1016/j.bios.2013.10.026.

References

Abad, J.M., Vélez, M., Santamariá, C., Guisán, J.M., Matheus, P.R., Vázquez, L., Gazaryan, I., Gorton, L., Gibson, T., Fernández, V.M., 2002. J. Am. Chem. Soc. 124, 12845–12853.
Akanda, M.R., Aziz, M.A., Jo, K., Tamilavan, V., Hyun, M.H., Kim, S., Yang, H., 2011. Anal. Chem. 83, 3926–3933.
Akanda, M.R., Choe, Y.-L., Yang, H., 2012. Anal. Chem. 84, 1049–1055.
Akanda, M.R., Tamilavan, V., Park, S., Jo, K., Hyun, M.H., Yang, H., 2013. Anal. Chem. 85, 1631–1636.
Cissell, K.A., Shrestha, S., Deo, S.K., 2007. Anal. Chem. 79, 4754–4761.
Das, J., Aziz, M.A., Yang, H., 2006. J. Am. Chem. Soc. 128, 16022–16023.
Das, J., Jo, K., Lee, J.W., Yang, H., 2007. Anal. Chem. 79, 2790–2796.
Deore, B.A., Freund, M.S., 2005. Chem. Mater. 17, 2918–2923.
Dong, H., Jin, S., Ju, H., Hao, K., Xu, L.-P., Lu, H., Zhang, X., 2012. Anal. Chem. 84, 8670–8674.
Dong, H., Lei, J., Ding, L., Wen, Y., Ju, H., Zhang, X., 2013. Chem. Rev. 113, 6207–6233.
Duan, R., Zuo, X., Wang, S., Quan, X., Chen, D., Chen, Z., Jiang, L., Fan, C., Xia, F., 2013. J. Am. Chem. Soc. 135, 4604–4607.
Frasconi, M., Tel-Vered, R., Riskin, M., Willner, I., 2010. Anal. Chem. 82, 2512–2519.
Gao, Z., 2012. The Analyst 137, 1674–1679.
Gao, Z., Deng, H., Shen, W., Ren, Y., 2013. Anal. Chem. 85, 1624–1630.
Gao, Z., Yu, Y.H., 2007. Biosensors Bioelectron. 22, 933–940.
Gao, Z.Q., Yang, Z.C., 2006. Anal. Chem. 78, 1470–1477.
Ho, J.A., Hsu, W.-L., Liao, W.-C., Chiu, J.-K., Chen, M.-L., Chang, H.-C., Li, C.-C., 2010. Biosensors Bioelectron. 26, 1021–1027.
Hong, C.-Y., Chen, X., Liu, T., Li, J., Yang, H.-H., Chen, J.-H., Chen, G.-N., 2013. Biosensors Bioelectron. 50, 132–136.
Johnson, B.N., Mutharasan, R., 2012. Anal. Chem. 84, 10426–10436.
Kanayama, N., Kitano, H., 2000. Langmuir 16, 577–583.
Kanekiyo, Y., Naganawa, R., Tao, H., 2004. Chem. Commun., 1006–1007.
Kilic, T., Topkay, S., Ozsoz, M., 2013. Biosensors Bioelectron. 48, 165–171.
Kilic, T., Topkaya, S.N., Ariksoysal, D.O., Ozsoz, M., Ballar, P., Erac, Y., Gozen, O., 2012. Biosensors Bioelectron. 38, 195–201.
Lévy, R., Thanh, N.T.K., Doty, R.C., Hussain, I., Nichols, R.J., Schiffrin, D.J., Brust, M., Fernig, D.G., 2004. J. Am. Chem. Soc. 126, 10076–10084.
Lee, J.M., Jung, Y., 2011. Angew. Chem. Int. Ed. 50, 12487–12490.

Li, H., Liu, Y., Liu, J., Liu, Z., 2011. Chem. Commun. 47, 8169–8171.
Lin, P.-C., Chen, S.-H., Wang, K.-Y., Chen, M.-L., Adak, A.K., Hwu, J.-R.R., Chen, Y.-J., Lin, C.-C., 2009. Anal. Chem. 81, 8774–8782.
Lin, Z., Pang, J., Yang, H., Cai, Z., Zhang, L., Chen, G., 2011. Chem. Commun. 47, 9675–9677.
Liu, L., Deng, D., Xing, Y., Li, S., Yuan, B., Chen, J., Xia, N., 2013a. Electrochim. Acta 89, 616–622.
Liu, L., Du, J., Li, S., Yuan, B., Han, H., Jing, M., Xia, N., 2013b. Biosensors Bioelectron. 41, 730–735.
Liu, L., He, Q., Zhao, F., Xia, N., Liu, H., Li, S., Liu, R., Zhang, H., 2014. Biosensors Bioelectron. 51, 208–212.
Lu, Y., Li, X., Zhang, L., Yu, P., Su, L., Mao, L., 2008a. Anal. Chem. 80, 1883–1890.
Lu, Z., Liu, M., Stribinskis, V., Klinge, C.M., Ramos, K.S., Colburn, N.H., Li, Y., 2008b. Oncogene 27, 4373–4379.
Lusi, E.A., Passamano, M., Guarascio, P., Scarpa, A., Schiavo, L., 2009. Anal. Chem. 81, 2819–2822.
Moreno-Guzmán, M., Ojeda, I., Villalonga, R., González-Cortés, A., Yáñez-Sedeño, P., Pingarrón, J.M., 2012. Biosensors Bioelectron. 35, 82–86.
Nelson, P.T., Baldwin, D.A., Scearce, L.M., Oberholtzer, J.C., Tobias, J.W., Mourelatos, Z., 2004. Nat. Methods 1, 155–161.
Pöhlmann, C., Sprinzl, M., 2010. Anal. Chem. 82, 4434–4440.
Paleček, E., Bartošík, M., 2012. Chem. Rev. 112, 3427–3481.
Peng, Y., Gao, Z., 2011. Anal. Chem. 83, 820–827.
Pham, T.A., Kumar, N.A., Jeong, Y.T., 2010. Colloids Surf. A: Physicochem. Eng. Aspects 370, 95–101.
Potter, O.G., Breadmore, M.C., Hilder, E.F., 2006. The Analyst 131, 1094–1096.
Rahman, M.M., Elaissari, A., 2012. Drug Discov. Today 17, 1199–1207.
Ren, Y., Deng, H., Shen, W., Gao, Z., 2013. Anal. Chem. 85, 4784–4789.
Schmittgen, T.D., Jiang, J., Liu, Q., Yang, L., 2004. Nucleic Acids Res. 32, e43.
Shen, W., Deng, H., Ren, Y., Gao, Z., 2013. Biosensors Bioelectron. 44, 171–176.
Shimomura, M., Abe, T., Sato, Y., Oshima, K., Yamauchi, T., Miyauchi, S., 2003. Polymer 44, 3877–3882.
Song, S.Y., Han, Y.D., Park, Y.M., Jeong, C.Y., Yang, Y.J., Kim, M.S., Ku, Y., Yoon, H.C., 2012. Biosensors Bioelectron. 35, 355–362.
Streit, S., Michalski, C.W., Erkan, M., Kleef, J., Friess, H., 2009. Nat. Protocols 4, 37–43.
Tang, J., Tang, D., Su, B., Huang, J., Qiu, B., Chen, G., 2011. Biosensors Bioelectron. 26, 3219–3226.
Tosar, J.P., Brañas, G., Laíz, J., 2010. Biosensors Bioelectron. 26, 1205–1217.
Tran, H.V., Piro, B., Reisberg, S., Tran, L.D., Duc, H.T., Pham, M.C., 2013. Biosensors Bioelectron. 49, 164–169.
Trefulka, M., Bartošík, M., Paleček, E., 2010. Electrochem. Commun. 12, 1760–1763.
Walter, A., Wu, J., Flechsig, G.-U., Haake, D.A., Wang, J., 2011. Anal. Chim. Acta 689, 29–33.
Wang, J., Yi, X., Tang, H., Han, H., Wu, M., Zhou, F., 2012. Anal. Chem. 84, 6400–6406.
Wang, Z., Lévy, R.I., Fernig, D.G., Brust, M., 2005. Bioconjugate Chem. 16, 497–500.
Wang, Z.W., Zhang, J., Guo, Y., Wu, X.Y., Yang, W.J., Xu, L.J., Chen, J.H., Fu, F.F., 2013. Biosensors Bioelectron. 45, 108–113.
Xia, N., Deng, D., Zhang, L., Yuan, B., Jing, M., Du, J., Liu, L., 2013a. Biosensors Bioelectron. 43, 155–159.
Xia, N., Zhang, L., Wang, G., Feng, Q., Liu, L., 2013b. Biosensors Bioelectron. 47, 461–466.
Xie, H., Zhang, C., Gao, Z., 2004. Anal. Chem. 76, 1611–1617.
Yang, H., 2012. Curr. Opinion Chem. Biol. 16, 422–428.
Yang, H., Hui, A., Pampalakis, G., Soleymani, L., Liu, F.F., Sargent, E.H., Kelley, S.O., 2009. Angew. Chem. Int. Ed. 48, 8461–8464.
Yin, H., Zhou, Y., Chen, C., Zhu, L., Ai, S., 2012a. The Analyst 137, 1389–1395.
Yin, H., Zhou, Y., Zhang, H., Meng, X., Ai, S., 2012b. Biosensors Bioelectron. 33, 247–253.
Zayats, M., Katz, E., Willner, I., 2002. J. Am. Chem. Soc. 124, 14724–14735.
Zhang, G.J., Chua, J.H., Chee, R.E., Agarwal, A., Wong, S.M., 2009. Biosensors Bioelectron. 24, 2504–2508.
Zhou, Y., Wang, M., Meng, X., Yin, H., Ai, S., 2012a. RSC Adv. 2, 7140–7145.
Zhou, Y., Wang, M., Meng, X., Yin, H., Ai, S., 2012b. New J. Chem. 36, 1985–1991.